Contributed Papers from Materials Science and Technology 2017 (MS&T17)
October 8 – 12, 2017, David L. Lawrence Convention Center, Pittsburgh, Pennsylvania USA

DOI 10.7449/2017/MST_2017_454_462

Liquid Metal Embrittlement of Resistance Spot Welded 1180TRIP Steel - Effects of Crack Geometry on Weld Mechanical Performance

Du-Youl Choi[1], Sang-Ho Uhm[1], Charles M. Enloe[2], Hokook Lee[1], Gyosung Kim[1], Curt Horvath[2]

[1] POSCO Global R&D Center
Incheon 406-840, South Korea

[2] General Motors, LLC
GM Product Integrity, Body Structures & Closures Materials Engineering
Warren, MI 48092, USA

Keywords
Advanced High Strength Steel, Light-Weighting, Crashworthiness, Transformation Induced Plasticity, Liquid Metal Embrittlement

Abstract

Transformation Induced Plasticity (TRIP) steels exhibiting favorable combinations of strength and ductility have received much attention for automotive applications. However, challenges to resistance spot weldability of zinc-coated TRIP steel such as low energy fracture and liquid metal embrittlement (LME) have emerged and require resolution prior to full implementation in the vehicle body structure. In this study, resistance spot welding Zn-coated TRIP1180 (1180 MPa minimum ultimate tensile strength) steel was conducted to produce spot welds exhibiting various levels of surface cracking. Static strength and fatigue life in the tensile loading mode were then evaluated in cross tension orientation. No significant reduction in cross tension strength, absorbed energy, and fatigue life was observed for tested samples containing cracks less than 325 μm in comparison to the crack-free welds, but the performance of the spot welds exhibiting large LME cracks (> 500 μm) was significantly reduced.

Introduction

The competitive advantage of steel relative to alternative material solutions for automotive body structure applications is dependent upon significant strength increases for gauge reduction given current government and industry vehicle fuel efficiency and crash performance targets [1-2]. A continued increase in AHSS utilization, however, is reliant upon successful solution to manufacturing challenges separate from the underlying physical and process metallurgy for sheet steel production. Perhaps the most significant of the current impediments to complete implementation of TRIP steels within the vehicle body structure is development of an acceptable joining strategy for zinc-coated TRIP steel variants. The primary physical phenomenon that has hindered development of an acceptable joining strategy for a multitude of advanced steels, including zinc-coated TRIP steels, is the presence of liquid metal embrittlement of regions within or directly adjacent to resistance spot welds [3]. Combinations of enhanced steel hardenability due to the various alloy additions necessary for the production of TRIP steel and the individual effects of these alloying elements on liquid Zn behavior in proximity to grain boundaries results in significant susceptibility to liquid metal induced cracking during standard resistance spot welding.

Beyond confirmation of the presence of LME cracking and characterization of crack depth as a function of both material and welding parameters, a proper quantification of the effects of LME cracking on joint performance is needed for the range of loading geometries to be encountered in service. Previous investigations have demonstrated varying effects of LME cracking on joint performance, and it is noted that fatigue performance in tensile shear and cross tension loading is not significantly influenced by the presence of LME cracks in selected AHSS grades with ultimate tensile strengths below 1000 MPa [4-6]. In this study, the effects on spot weld joint performance of varying LME crack size and location are investigated in quasi-static tensile shear mode, cross-tension mode, and cross tension fatigue.

Experimental Procedure

Experimental Materials

An 1180 MPa minimum ultimate tensile strength TRIP (transformation induced plasticity) steel with a nominal composition of 0.17C-2.6Mn-1.5Si and thickness of 1.6 mm was chosen for investigation. The nominal uniaxial yield strength, ultimate tensile strength, and total elongation of the selected grade are 960 MPa, 1200 MPa, and 16%, respectively, as tested according to ASTM E8. An example microstructure of the selected commercially-produced steel containing ferrite, martensite, bainite, and retained austenite is shown in Figure 1.

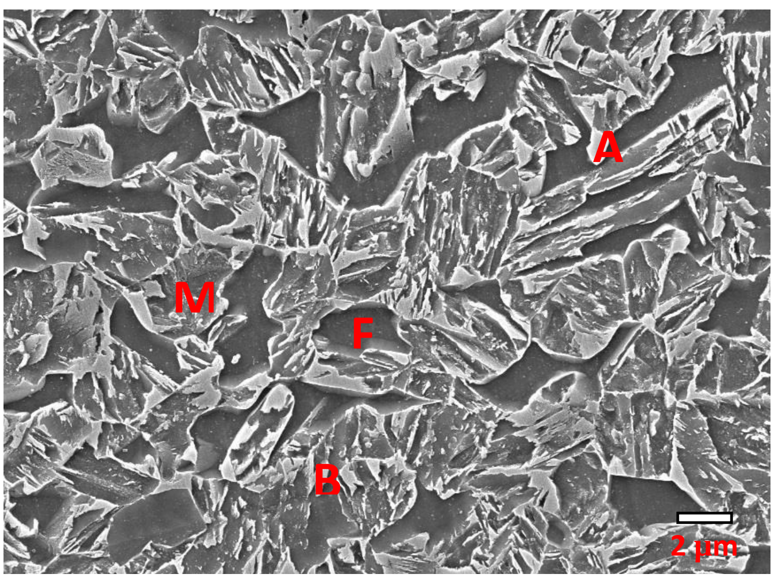

Figure 1. Representative scanning electron micrograph of the evaluated 1180 TRIP steel displaying a microstructure consisting of ferrite (F), martensite (M), bainite (B), and retained austenite (A).

To generate liquid metal embrittlement cracks of sufficiently varying size, two coating systems were employed on the 1180 TRIP steel substrate based on previous observation. Galvanized (GI) 1180 TRIP steel was employed for generation of LME cracks less than 300 μm in depth, and a Zn-Mg alloy coating (ZM) was employed for generation of LME cracks greater than 500 μm in depth within the 1180 TRIP substrate. Subsequently described welding parameters were chosen for test coupon preparation to generate a range of Type B LME crack depths within the ranges outlined above. Figure 2 shows the location and orientation of potential LME cracks, labeled Type A, Type B, or Type C, within the evaluated homogeneous (self-similar) 2-thickness weld coupons.

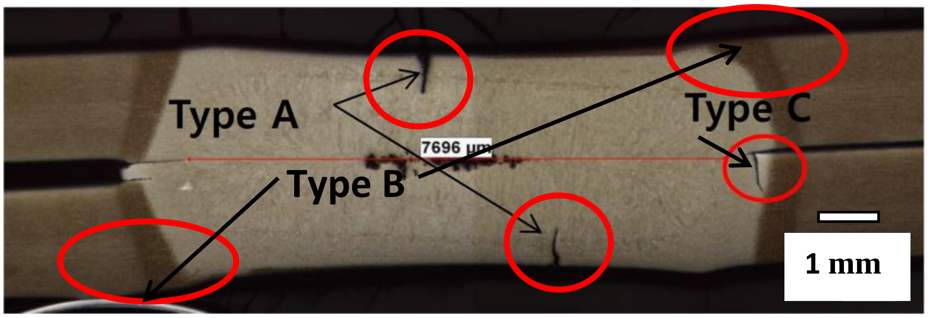

Figure 2. LME crack location and orientations possible within Zn-coated TRIP steel substrates: Type A cracks are located within the sheet/electrode contact surface; Type B cracks are location outside the sheet/electrode contact surface in the vicinity of the heat affected zone (HAZ); Type C cracks are located at the sheet-to-sheet contact interface. Type B and Type C cracks are primarily caused by liquid Zn, whereas Type A cracks are caused by the presence of both Zn and Cu.

Weld Test Coupon Preparation and LME Crack Characterization

Weld coupons of 1.6 mm 1180 TRIP steel (2 thickness joints) were fabricated by shearing specimens to the proper blank dimensions (125mm x 40mm for initial LME crack and tensile shear mechanical evaluation, and 150 mm x 50 mm for cross tension mechanical evaluations – both monotonic quasi-static loading and fatigue) and welding into either tensile shear or cross tension specimen geometries as shown in Figure 3. All weld specimens were fabricated using a medium frequency direct current welding with Cu-Cr-Cr electrodes (OD 16 mm, TD 6 mm) with an electrode force of 5.0 kN.

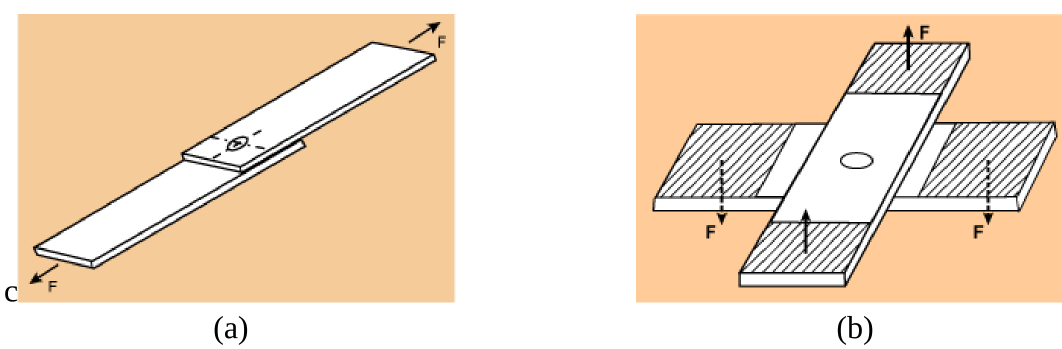

Figure 3. (a)Tensile shear and (b) cross tension sample loading schematics.

For initial observation and characterization of LME crack size as a function of weld parameters in GI 1180 TRIP, welding current was selected for various single pulse weld times as 0.5 kA less than expulsion current, i.e., I = 8.0 kA for 200 ms weld time, I = 6.5 kA for 400 ms weld time, and I = 6.5 kA for 800 ms weld time. Hold time times of 20, 300, and 1000 ms were then applied for each selected weld current-time combination. An outline of the described weld parameters is given in Table I.

Characterization of the generated LME cracks following welding according to the parameters listed in Table I was performed by liquid dye penetrant testing and metallographic examination of the weld joint at 0°, 45°, and 90° from the major axis of the weld coupons for direct comparison to dye penetrant testing and measurement of crack depth.

Table I – Weld Parameter Combinations for LME Observations in GI 1180 TRIP

Weld Time (ms)	Weld Current (kA)	Hold Times (ms)
200	8.0	20, 300, 1000
400	6.5	20, 300, <u>1000</u>
800	6.5	20, 300, <u>1000</u>

Based on initial LME crack size characterizations for GI 1180 TRIP, weld parameters were selected for generation of small (20-80 µm) and medium (100-250 µm) depth Type B cracks for subsequent mechanical evaluation in tensile shear, cross tension and cross tension fatigue (these conditions are indicated by underlined hold times in Table I). Crack-free samples were fabricated for mechanical performance comparison by chemical removal of the Zn-based coating and subsequent welding to achieve similar weld joint morphology utilizing the same base weld parameters as the comparison cracked samples. Large Type B LME cracks (>500 µm) were generated for mechanical evaluation and joint performance comparison by welding of ZM-coated 1180 TRIP steels using weld current, I = 6.5 kA, for 400 ms weld time and 1000 ms hold time.

<u>Mechanical Evaluation</u>

For preparation of tensile shear and cross tension sample configurations previously shown in Figure 3, weld parameters were selected as previously outlined for production of samples containing small (20-80 µm), medium (100-325 µm), and large (>500 µm) Type B LME cracks for mechanical evaluation. Following preparation, welded samples were tested tensile shear (crosshead speed = 10 mm/min), cross tension (crosshead speed = 10 mm/min), and cross tension fatigue (load amplitude = 1.0 kN, R = 0.1).

Results & Discussion

<u>LME Cracking – Optical Microscopy and Dye Penetrant Testing</u>

Optical microscopy and dye penetrant testing indicated several correlated trends with respect to weld parameters effects on the extent and depth of LME cracking in tested coupons. Figure 4 shows representative optical micrographs of evaluated weld conditions highlighting the effects of hold time on observed Type A, Type B, and Type C cracking for a fixed weld time of 800 ms. Stereoscopic images of dye penetrant results are included in Figure 4 for direct comparison to weld joint micrographs (shown at nominal magnifications of 12.5x for the complete weld joint and 100x for LME crack detail). Similar examinations were performed for weld times or 200 ms and 400 ms, but results are omitted here for brevity. Qualitatively, both the number and depth of Type A and Type B cracks increase as a function of weld time for a given hold time. Additionally, Type A cracking appears to be reduced with increased hold times, while Type C cracking appears at a combination of increased weld time and reduced hold time.

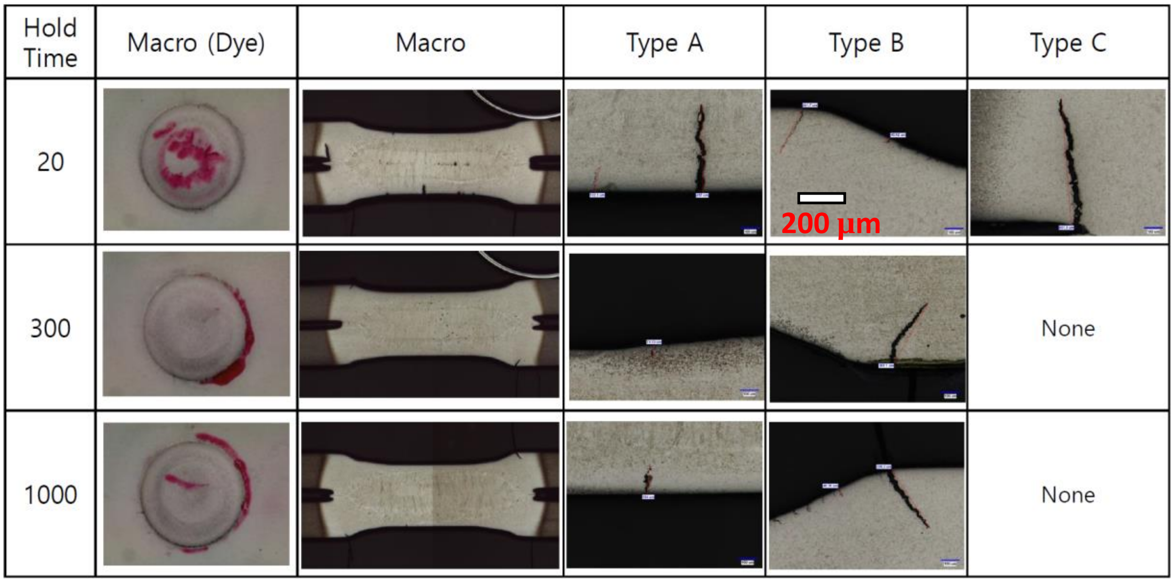

Figure 4. Macro-images of dye penetrant testing and optical micrographs of complete weld joint (12.5x) and LME crack detail (100x) for weld times (current) of 800 ms (6.5 kA). Hold times are provided in ms. Scale bar included for crack detail reference.

Quantification of the maximum observed maximum crack sizes of Types A, B, and C, and nugget diameter for the evaluated weld parameters is provided in Figure 5 as a function of weld time for various hold times. With increased weld time, measured nugget size increases in addition to electrode indentation depth. Increases in weld time also indicate a general increase in the maximum observed depth of Type B (and/or Type A and C) cracks. Type A cracking appears to coincide with both short and long hold times and is most prevalent for the longest tested welding time. Type C cracking is again noted to be initiated at long weld time and short hold time.

Mechanical Evaluations

Based on the crack measurements, GI 1180 TRIP samples were generated with small (20-80 µm) and medium (100-325 µm) Type B LME cracks for mechanical testing based on weld parameters outlined previously and indicated by red arrows in Figure 5(c). As previously noted, large cracks were generated by welding of ZM-coated 1180 TRIP test coupons, and crack free samples were generated by welding of uncoated 1180 TRIP. Measured crack depth ranges for evaluated test coupons utilizing the described conditions are shown in Table II.

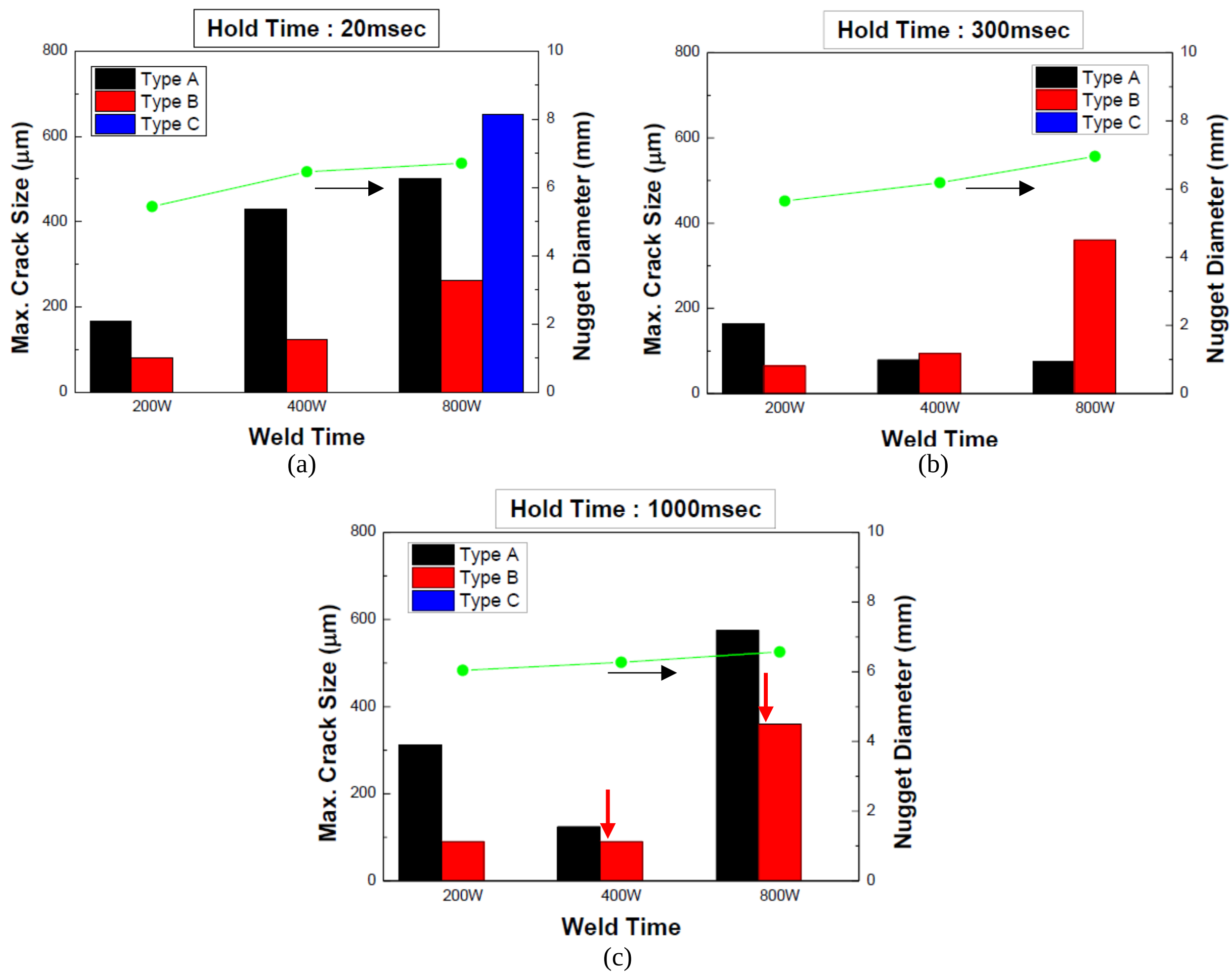

Figure 5. Maximum observed Type A, B, and C crack size (left axis) and measured average nugget diameter (right axis – data shown in green) as a function of weld time for weld hold times of (a) 20 ms, (b) 300 ms, and (c) 1000 ms. Red arrows in (c) indicate conditions chosen for generation of LME cracks for mechanical evaluation.

Comparative tensile shear load-displacement results are shown in Figure 6 for small Type B cracked samples. In the displayed load-displacement plot, cracked samples are shown in comparison to crack free samples welded under identical conditions. Similar load-displacement testing was conducted for medium and large crack-containing samples but is omitted here for brevity. No significant degradation in tensile shear performance was measured in samples exhibiting small and medium depth Type B cracks.

Comparative cross tension load-displacement results are shown in Figures 7 for small Type B cracked samples. In the displayed load-displacement plots, cracked samples are shown in comparison to crack free samples welded under identical conditions. Similar load-displacement testing was conducted for medium and large crack-containing samples but is omitted here for brevity. No significant degradation in cross tension load-displacement performance was measured in samples exhibiting small and medium depth Type B cracks.

Table II – Weld Parameters and Associated Type B Crack Depth and Nugget Size for Mechanically Tested Conditions

D	Coating	Weld Time (ms)	Hold Time (ms)	Nugget Dia. (mm)	Type B Crack Depth (μm)
S(Small)	GI	400	1000	6.32	27-80
M(Medium)	GI	800	1000	6.24	136-325
L(Large)	ZM	400	1000	5.65	642-757
SD	Bare	400	1000	6.41	0
MD	Bare	800	1000	6.25	0
LD	Bare	400	1000	5.73	0

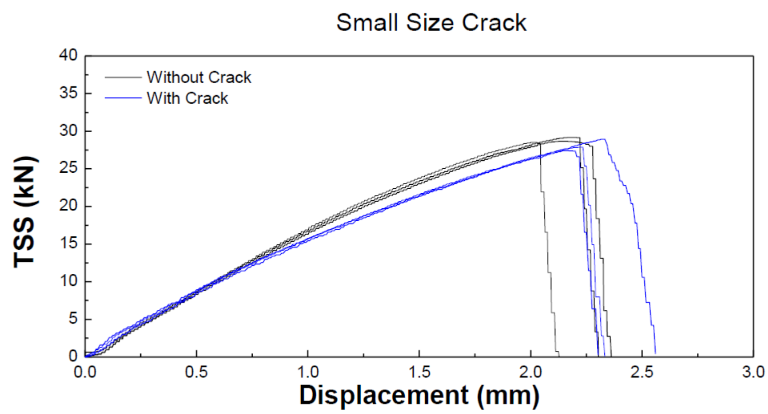

Figure 6. Tensile shear load-displacement curves for small (20-80 μm) crack containing (blue) relative to crack-free (black) specimens.

Comparative cross tension fatigue life results are shown in Table III for small Type B cracked samples, respectively, and a joint efficiency (JE) rating is calculated as the ratio of cycles to fatigue failure for the cracked samples relative to the average for crack free samples. Average measured nugget diameters (ND) for each condition are provided for reference. Similar fatigue testing was conducted for medium and large crack-containing samples but is omitted here for brevity. No significant degradation in cross tension fatigue performance was measured in samples exhibiting small and medium depth Type B cracks.

Tabulated parameters of interest (displacement at peak load, peak load, and energy absorbed to fracture, and cross tension fatigue life) from individual test results described above were extracted, and a joint efficiency (JE) rating was calculated as the ratio of the average parameter for the Type B LME cracked samples relative to the average for crack free samples. Joint efficiency ratings for small, medium, and large Type B cracked specimens are compiled from previously outlined results and shown in Figure 8. Data indicate that joints welded with parameters known to exhibit LME cracking less than ~325 μm, i.e., medium crack size or smaller, show no significant degradation in performance (JE >90%) as a result of LME crack presence within the evaluated sample set.

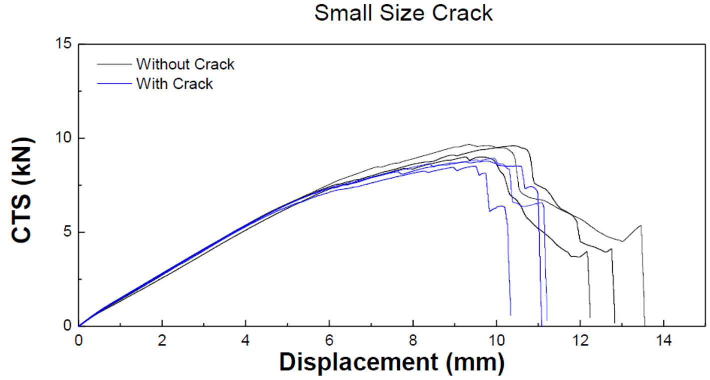

Figure 7. Cross tension load-displacement curves for small (20-80 µm) crack-containing (blue) relative to crack-free (black) specimens.

Table III – Cross Tension Fatigue Life of Small Type B Cracked Specimens

LME Crack Condition		Crack Free	Type B Small (<80 µm)
Nugget Diameter (mm)		6.41	6.32
Fatigue Life (cycles)	1	398,186	453,684
	2	392,660	501,917
	3	556,493	565,380
	Average	449,113	506,994
JE (%)		-	113

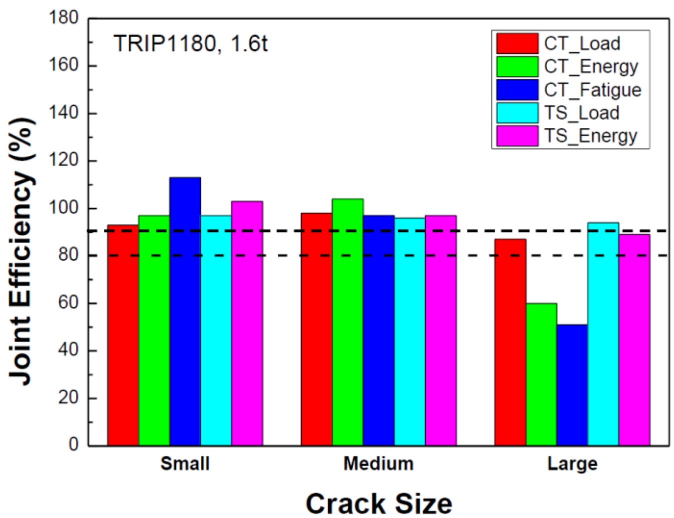

Figure 8. Compiled joint efficiency ratings for small, medium, and large Type B crack-containing spot welds measured by tensile shear (TS) and cross tension (CT) peak load, absorbed energy, and cycles to fatigue failure.

Summary

Significant performance reductions of homogeneous Zn-coated 1180 TRIP spot welds as measured by tensile shear and cross tension strength, absorbed energy in tensile shear and cross tension, and fatigue life were observed for tested samples containing LME cracks less than 500 μm in comparison to the crack-free welds, but the performance of resistance spot welds exhibiting small to medium LME cracks (depths < 325 μm) was not significantly reduced.

References

1. Vol. 78, No. 206 Fed. Reg. 73478 (October 26, 2016) (to be codified at 40 CFR Parts 9, 22, 85, 86, 600, 1033, 1036, 1037, 1039, 1042, 1043, 1065, 1066, and 1068).
2. CAFE – Corporate Average Fuel Economy (n.d.). US Department of Transportation. [Online]. Available: https://www.nhtsa.gov/laws-regulations/corporate-average-fuel-economy
3. C. D. Horvath et al., "Persistent Challenges to Advanced High-Strength Steel Implementation," in Proceedings of the International Symposium on New Developments in Advanced High-Strength Sheet Steel, Keystone, CO, AIST (2017), pp.1-10.
4. Y. Kim et al., "Evaluation of Surface Crack in Resistance Spot Welds of Zn-Coated Steel," *Materials Transactions*, Vol. 55, No. 1, pp. 171-175 (2014).
5. B. Yan et al., "Spot weld fatigue of dual phase steels," Proceedings of the SAE 2004 World Congress, Detroit, MI, SAE International (2004). 2004-01-0511
6. H. Gaul et al., "Influence of HAZ cracks on fatigue resistance of resistance spot welded joints made of advanced high strength steels", *Science and Technology of Welding and Joining*, Vol. 16, No. 5, pp. 440-445 (2011).